ACS Catalysis

Research Article

pubs.acs.org/acscatalysis

Strong π-Acceptor Ligands in Rhodium-Catalyzed Hydroformylation of Ethene and 1-Octene: Operando Catalysis

Olivier Diebolt, Hugo Tricas,[‡] Zoraida Freixa,[§] and Piet W. N. M. van Leeuwen*

Institute of Chemical Research of Catalonia (ICIQ), Av. Paisos Catalans, 16, 43007 Tarragona, Spain

Supporting Information

ABSTRACT: Strong π-acceptor *N*-pyrrolylphosphoramidite and pyrrolylphosphine mono- and bidentante ligands were applied in ethene hydroformylation using a stoichiometric gas mixture CO/H_2/ethene 1:1:1. Very fast reactions (TOF up to 29.5×10^3 mol mol^{-1} h^{-1}, 13-fold faster than triphenylphosphine) and excellent selectivities were obtained. The pyrrolylphosphine derivatives of SPANphos and Xantphos, pySPAN and pyXANT, were used in 1-octene hydroformylation. The electronic character of these ligands improved both activities and regioselectivities compared with the phenyl-substituted ligands. HPNMR and HPIR showed that both pySPAN and pyXANT favor the formation of bisequatorial $[RhH(CO)_2(ligand)]$ complexes under catalytic conditions.

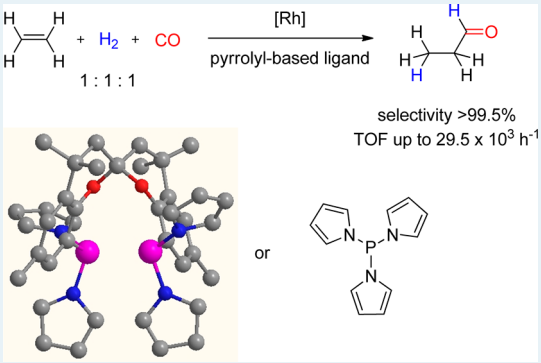

KEYWORDS: *in situ spectroscopy, π-accepting phosphorus ligands, rhodium, ethene, hydroformylation*

INTRODUCTION

For several decades, the hydroformylation of alkenes has been one of the most important reactions in industry employing homogeneous catalysts. The first applied industrial processes used a cobalt catalyst. Later, it was found that rhodium catalysts in combination with phosphorus donor ligands can lead to enhanced activity and selectivity.[1,2] The mechanism was postulated to be similar to the one described by Heck and Breslow for the cobalt system, in which monometallic penta-coordinated hydrides are the starting point of the catalytic cycle.[3] During subsequent decades, extensive work has been performed on the development of phosphorus-based ligands to improve the catalytic activity as well as chemo- and regio-selectivity.[4−8] In particular, the use of phosphite ligands has been the focus of many reports,[9] following their introduction by Pruett and Smith.[10] Compared with arylphosphine ligands, their better π-accepting character resulted in a higher activity toward nonactivated alkenes. Bulky monophosphites first received attention from Van Leeuwen and Roobeek,[11] whereas Bryant and co-workers at Union Carbide reported major breakthroughs with the use of diphosphites.[12] The bulky tris(*o*-*tert*-butyl-*p*-methylphenyl)phosphite (Figure 1) led to rates of reaction at least 10 times higher than conventional triphenylphosphine-modified rhodium precursors.[13] The highest reported rate for 1-octene hydroformylation with the use of this ligand is 85.5×10^3 h^{-1}, and this catalytic system also showed remarkable activity toward other olefins, such as cyclohexene and styrene.[14] Moreover, this phosphite displayed very good properties for ethene hydroformylation: low price, high stability, very high selectivity toward propanal, and high reaction rate at 80 °C (TOF = 16.7×10^3 h^{-1} at [Rh] = 0.25 mM).[15] Notably, other bulky monophosphite ligands showed activity up to 34.7×10^3 h^{-1} (at 10 bar of ethene), but their lower stabilities toward hydrolysis and their higher costs preclude industrial applications.

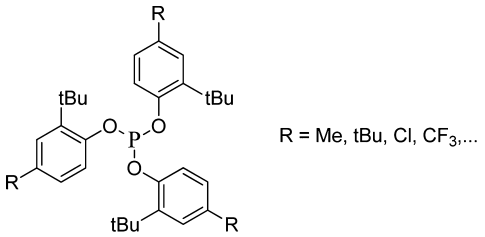

Figure 1. Bulky phosphites developed by van Leeuwen and co-workers.

The outstanding electronic effect of these ligands resulted in a general interest in strong π-acceptor ligands. In addition to phosphites, phosphabenzenes and pyrrolyl-based phosphorus ligands (Figure 2) also received ample attention.[16−20] These new classes of ligands have found application in homogeneous catalysis, particularly in rhodium-catalyzed hydroformylation.[21−30] More recently, a bidentate pyrrolyl-based ligand possessing a xanthene backbone (pyXANT, vide infra) was reported to display excellent activity and chemo- and regioselectivity in the related hydroaminomethylation reaction of a terminal olefin. This tandem reaction involves a hydroformylation in situ, followed by a reductive amination with a primary or secondary amine.[31]

Received: July 16, 2012
Revised: December 4, 2012
Published: December 6, 2012

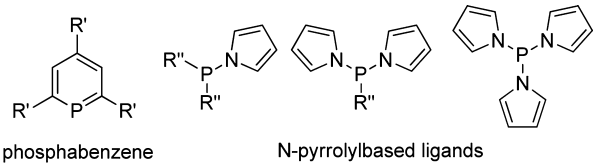

Figure 2. Phosphabenzenes and pyrrolyl-based phosphorus ligands.

The hydroformylation of ethene, leading to propanal and 1-propanol, is a reaction of industrial interest because these chemical compounds can find many applications. In addition to their direct use as solvents, they are also important intermediates for the production of pesticides, pharmaceuticals, and fragrances, and potentially propene. Many examples, including heterogeneous catalytic systems, were reported for this reaction. Notably, the group of Cole-Hamilton reported the excellent activity and selectivity toward *n*-propanol using a triethylphosphine-modified rhodium catalyst, achieving turnover frequencies up to 54 × 10^3 h^{-1},[32] The mechanism and kinetics of ethene rhodium-catalyzed hydroformylation have been extensively studied in the last 20 years,[33−35] and intermediate species such as $[HRh(CO)_3(\eta^2\text{-ethene})]$[33] and $[CH_3CH_2C(=O)Rh(CO)_4]$[34] were detected, but to the best of our knowledge, no systematic study of ligand effects has been reported.

We report here the synthesis of pyrrolyl-based mono- and bidentate ligands and their application in ethene hydroformylation. For comparison, some related phosphines have been applied under the same conditions to emphasize the positive electronic effect.

Rhodium catalysts modified with bidentate ligands have also been investigated in 1-octene hydroformylation to determine the influence of the electronic properties of the ligands on the activity and regioselectivity. Their coordination properties in rhodium complexes have been studied by means of in situ spectroscopy under argon and at high pressure of syngas.

LIGANDS SYNTHESES

A wide range of pyrrolyl-based phosphorus ligands were synthesized to determine the influence of the steric properties of the ligand on the catalytic outcome. Pyrrolyl-based monodentate ligands were synthesized by reacting chlorophosphite (**L1−L6**),[36] dichlorophenylphosphine (**L7−L8**) or phosphorus trichloride (**L9−L10**) and the corresponding pyrrole in the presence of triethylamine in THF. Subsequent filtration to remove triethylammonium chloride and recrystallization afforded the pure compounds **L1−L10** (Figure 3). To show the general effect of π-accepting ligands on the hydroformylation rate, the pyrrolyl analogs of the well-known bidentate Xantphos[37] and SPANphos[38] were also synthesized. In this case, bis(1-pyrrolyl)chlorophosphine was reacted with the lithiated backbone of the corresponding ligand (Figure 4).

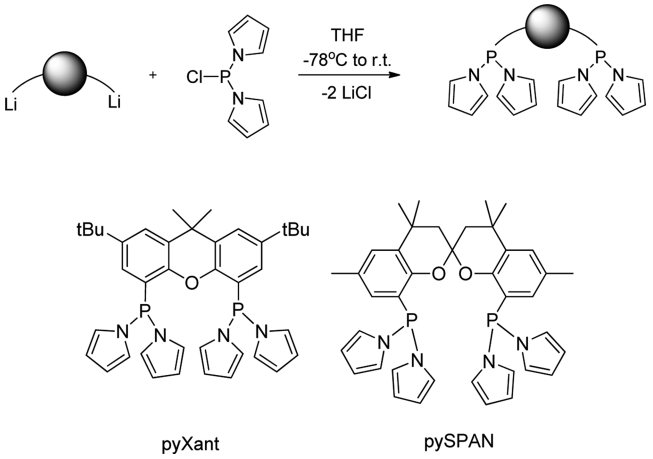

Figure 4. General synthesis of pyrrolyl analogs of Xantphos[39] and SPANphos.[36]

APPLICATION OF THE LIGANDS IN RHODIUM-CATALYZED HYDROFORMYLATION OF ETHENE

Pyrrolyl-Based Monodentate Ligands in Ethene Hydroformylation. The monodentate pyrrolyl-based phosphorus ligands described above were tested in ethene

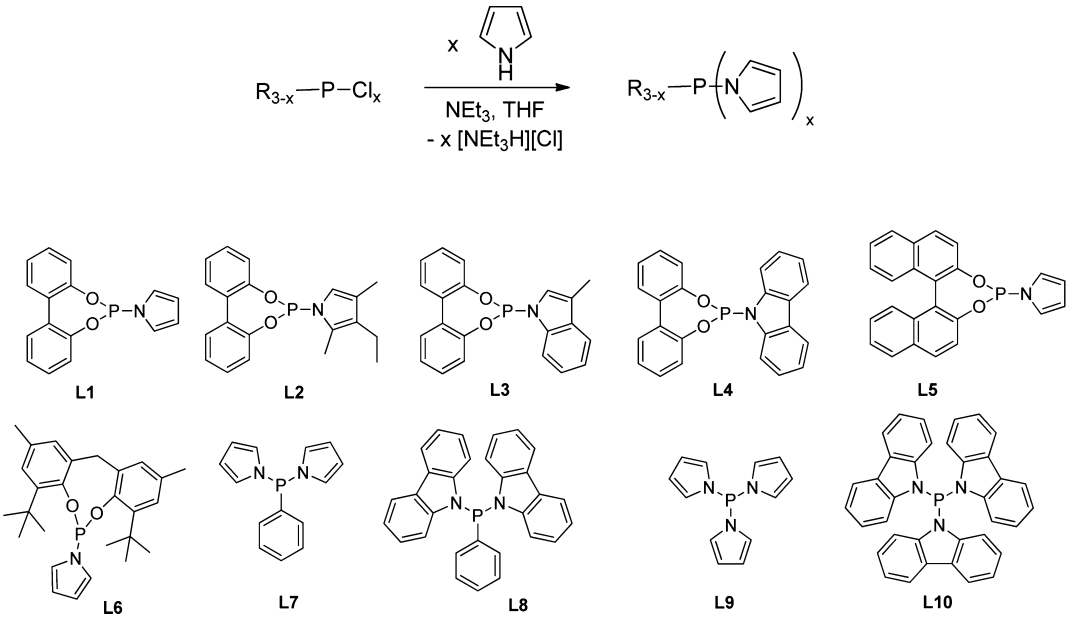

Figure 3. General synthesis of pyrrolyl-based monophosphines, amidites, and amides **L1−L10**.

dx.doi.org/10.1021/cs300470u | *ACS Catal.* 2013, 3, 128−137

hydroformylation at 80 °C using a stoichiometric gas ratio for ethene/CO/H_2 of 1:1:1 and a total gas pressure of 20 bar. Results are shown in Figure 5. As expected on the basis of their

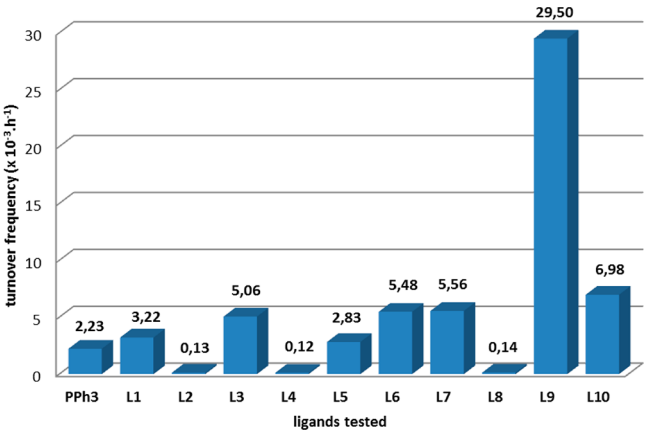

Figure 5. Initial TOF in ethene hydroformylation. Rh precursor [Rh(acac)$(CO)_2$]. Reaction in toluene at 80 °C. [Rh] = 0.25 mM. L/Rh = 20. $P_{(E/CO/H_2=1:1:1)}$ = 20 bar.

electronic properties, most of them showed higher activity than the conventional triphenylphosphine system. Importantly, all of them displayed excellent chemoselectivity, and propanal was the only species detected by gas chromatography. Ligands **L1**−**L4** bearing a biphenol moiety allow for comparison of the different types of N-heterocyclic substituents. **L1**, bearing pyrrole, is very active (1.5-fold more active than PPh_3), whereas **L2**, substituted with 2,4-methyl-3-ethylpyrrole, showed very low activity. This latter ligand is expected to be a slightly stronger σ-donor because of the presence of alkyl chains on the pyrrole ring, which can explain this lower activity. Comparison with the more active and more bulky carbazoyl-containing ligands seems to indicate that steric bulk in **L2** plays no role. **L3** induced very high activity (TOF = 5.1 × 10^3 h^{-1}), showing the beneficial effect of the 3-methylindole substituent. The carbazole substituent of **L4** decreased the activity of the catalytic system. This effect was previously observed by Beller in 2-pentene hydroformylation.[24] Binaphthol-substituted ligand **L5** shows an activity very comparable to that of **L1**, which is in agreement with their similar steric and electronic properties. Interestingly, the more bulky ligand **L6** leads to very high activity, showing the beneficial effect of steric hindrance in this case. Bis(pyrrolyl)phenylphosphine **L7**, which has even stronger π-accepting properties than phosphites, also provided high activity. Replacing the pyrrolyl by carbazoyl, ligand **L8**, led again to a drastic decrease in activity. With the aim to see the effect of strongly π-accepting ligands, tri(pyrrolyl)phosphine **L9** was tested. Gratifyingly, this ligand led to one of the most active catalytic systems reported for this transformation, with a turnover frequency of 29.5 × 10^3 h^{-1}. Tris(carbazoyl)phosphine, **L10**, showed significantly lower activity in this case, although the TOF is still relatively high. The strongest π-acceptor ligands, **L9** and **L10**, showed the highest activity. Ligands containing three pyrrole groups give more active catalysts than the ones containing a bisphenol group (cf. **L4** and **L10**), in line with the electronic parameters.[23]

Unfortunately, it was noticed that although ligand **L9** gave the highest initial TOF, it is also the one for which the reaction rate decreases the fastest. In our experimental setup, the reaction was kept at constant pressure by replenishing the autoclave to the set value at fixed time intervals. The TOFs shown are related to the gas consumption. Importantly, in the case of **L9**, TOF values decrease with time, showing perhaps (vide supra) the lower stability of the catalytic system based on this ligand (Figure 6). Note that the decay of the rate is not due to the

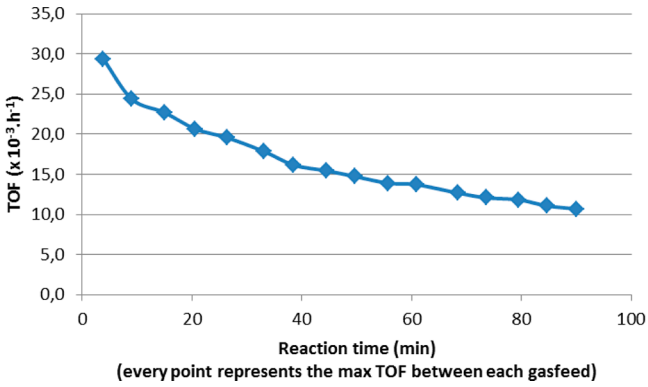

Figure 6. Evolution of the TOF using the catalytic system Rh−**L9**.

usual decrease in alkene concentration, as is the case for 1-octene hydroformylation, given its first-order dependence on substrate. Although the autoclave was automatically repressurized every 5−6 min, for **L9**, the reaction was so fast that the pressure decreased significantly between two gas feed cycles, which not only leads to lower rates but can also lead to faster catalyst decomposition. Thus, a continuous feed will lead to even faster reactions and probably also to a more stable catalyst. Alternatively, in part, the decreasing rate may be caused by deviations in the gas composition of the added mixture, which accumulate with each replenishment.

One might wonder whether a phosphine ligand-free species such as $HRh(CO)_3$ is responsible for the slow catalysis for **L3**, **L5**, and **L8**, as sometimes very bulky and electron-poor ligands do not coordinate under hydroformylation conditions;[40] however, these ligands are neither the most bulky nor the most electron-poor in the series tested, and thus, there must be other reasons for this.

Pyrrolylphosphine Bidentate Ligands in Ethene Hydroformylation. Bidentate phosphine ligands may lead to more stable catalyst systems. Usually bidentate ligands give lower rates of hydroformylation than monodentate ligands, but the low steric hindrance of ethylene compared with the usual substrates 1-octene or styrene may have an accelerating effect. To this end, the bispyrrolyl analogues of two well-known wide-bite angle diphosphines, Xantphos and SPANphos, were prepared as described above.

PyXANT and pySPAN were investigated in ethene hydroformylation under the same conditions utilized in the screening of the ligands used so far. The results were compared to those of their phenyl analogs Xantphos and SPANphos together with triphenylphosphine. The results, shown in Figure 7, demonstrate that pyrrolyl-modified bidentate ligands present a positive effect in rhodium-catalyzed ethene hydroformylation when compared with their diphenyl counterparts. The turnover frequency (TOF) values obtained with pyXANT and pySPAN are about 6−7 times higher than those of their phenyl analogs and close to the one obtained under the same conditions with tri(pyrrolyl)phosphine **L9** (vide infra).

Unexpectedly, the reaction rate decreases with time (Figure 8), but the decomposition seems to proceed more slowly than that of

dx.doi.org/10.1021/cs300470u | ACS Catal. 2013, 3, 128−137

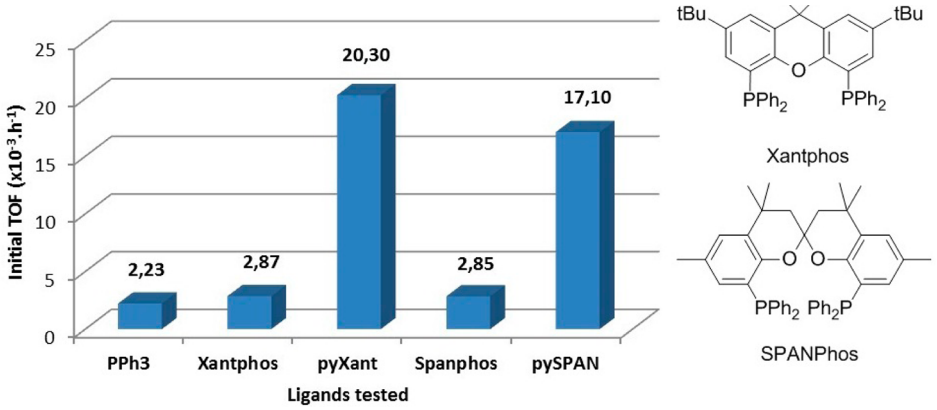

Figure 7. Initial TOF in ethene hydroformylation. Rh precursor [Rh(acac)$(CO)_2$]. Reaction in toluene at 80 °C. [Rh] = 0.25 mM. L/Rh = 20. $P_{(E/CO/H_2=1:1:1)}$ = 20 bar.

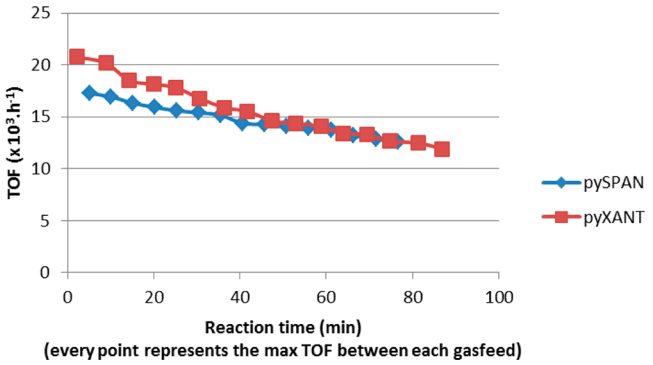

Figure 8. Evolution of the TOF using the pyXANT or pySPAN.

systems using **L9** (activity decay after 1 h of reaction 21 and 32% for pySPAN and pyXANT, respectively, compared with 54% for **L9**).

BIDENTATE PYRROLYL LIGANDS IN 1-OCTENE HYDROFORMYLATION. COMPARISON WITH PHENYL-SUBSTITUTED XANTPHOS AND SPANPHOS

Wide-bite angle bidentate ligands have shown their potential as modifying ligands for chemo- and regioselective rhodium-catalyzed hydroformylation of 1-alkenes.[41−50] In addition, π-accepting ligands were shown to give higher reaction rates and lower alkane formation. In some cases, a drawback of these ligands can be their high propensity for isomerization of 1-alkenes. Although this may be a disadvantage for terminal alkene hydroformylation, it can be used advantageously to convert internal alkenes to linear aldehydes.[44] These considerations led us to test the ligands pyXANT and pySPAN in 1-octene hydroformylation.

As above for ethene hydroformylation, the activities and selectivities obtained were compared with the parent SPANphos- and Xantphos-modified rhodium catalysts. The results are given in Table 1. The backbone effect observed for Xantphos and SPANphos was also seen for pyrrolyl-modified ligands. For instance, ligands with a xanthene backbone give high *l*/*b* ratios (entries 1 and 2), whereas bichromane backbone ligands gave lower regioselectivities (entries 3 and 4; for comparison, triphenylphosphine-modified catalysts give an *l*/*b* ratio of ∼3). All pyrrolyl-modified ligands led to higher *l*/*b* ratios and reaction rates than their phenyl-modified counterparts.

Table 1. 1-Octene Hydroformylation with Bidentate Ligands[a]

entry	ligand	TOF[b]	isomerization	*l*/*b* ratio	conversion[d]
1	pyXANT	1160	5.0	88	99.4
2	Xantphos	585	2.8	34.4	44.9
3	pySPAN	1360	12.5	6.4	98.2
4	SPANphos	500	4.1	2.4	90.0
5[c]	pyXANT	1250	2.0	104.1	98.7

[a]Reaction conditions: S/Rh = 1000; L/Rh = 20; [S] = 1.0 M in toluene; decane 0.2 M as internal standard; 20 bar syngas; 80 °C; reaction time, 90 min. (Catalyst preformation: 10 bar syngas, 80 °C, 90 min, and subsequent substrate addition under these conditions). [b]Initial turnover frequencies in mol mol^{-1} h^{-1}. [c]Syngas pressure is 40 bar. [d]Determined by GC analysis at the end of the reaction.

Although small steric effects cannot be excluded,[24,51] these important improvements in regioselectivity and rate must be attributed to electronic effects. In particular, the initial TOF is typically 2−3 fold higher for the pyrrolyl-substituted ligands (compare entries 1 and 3 with entries 2 and 4). Notably, the activity displayed by the Xantphos system decreases much faster with time than any other ligand, leading to incomplete conversion. Importantly, increasing the reaction pressure led to suppression of isomerization and a slight improvement of the regioselectivity (Table 1, entry 5). The high selectivities obtained with pyXANT as the ligand are comparable to those obtained with bisphenol-based pyrrolyl amidites, but the latter afford much faster catalysts.[23]

Electron-poor phosphorus ligands may be sensitive to hydrolysis of the pyrrolyl groups. Therefore, we studied the hydrolysis of **L7** as a model for pyXANT and pySPAN ligands and found that in neutral media, **L7** was surprisingly stable. In acidic media, complete decomposition was observed within 1 day (see the Supporting Information). Thus, the acids formed during decomposition need to be removed, as in phosphite-based catalysts.[52]

COORDINATION CHEMISTRY OF THE BIDENTATE LIGANDS

SPANphos and PySPAN. The crystal structure of pySPAN was obtained by X-ray diffraction of a single crystal. Selected bond distances and angles are described in Figure 9 and are compared with the data of unmodified SPANphos. The X-ray structure of pySPAN is very similar to that of SPANphos. The only differences between the structures are the slightly shorter

dx.doi.org/10.1021/cs300470u | ACS Catal. 2013, 3, 128−137

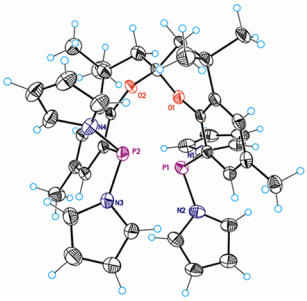

	PySPAN	SPANphos[38]
O—O (Å)	2.301	2.324
P—P (Å)	4.547	4.990
C—P (Å)	1.831	1.838
	1.811	1.836

Figure 9. Molecular structure of pySPAN as determined by X-ray diffraction. Thermal ellipsoids are shown at 50% probability. Selected interatomic distances of pySPAN and SPANphos ligands.

C−P bonds in pySPAN and the wider bite distance (P−P) in SPANphos.

Since both ligands present similar solid state structures, they are also expected to present coordination behavior similar to rhodium, neglecting electronic effects. Several comparative coordination studies toward different rhodium precursors have been performed,

It is known that SPANphos forms selectively mono- or dinuclear rhodium complexes with $[Rh(CO)_2Cl]_2$, depending only on the ligand-to-rhodium ratio employed.[53] When pySPAN was reacted with 0.5 equiv of the rhodium dimer, a mononuclear rhodium complex was formed, and when it was reacted with 1 equiv, a dinuclear complex was observed. The $^{31}P\{^1H\}$ NMR spectroscopic details of both compounds are compared with those of SPANphos analogs in Figure 10.

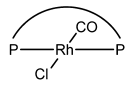

mononuclear	δ (ppm)	$^1J_{Rh-P}$ (Hz)	$^2J_{P-P}$ (Hz)
SPANphos[8]	22.3	365.4	132.0
	26.5	365.4	132.0
pySPAN	81.2	580.5	163.2
	93.5	580.5	163.2

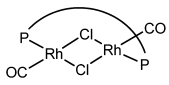

dinuclear	δ (ppm)	$^1J_{Rh-P}$ (Hz)
SPANphos[8] (*d*)	45.9	178.2
pySPAN (*d*)	106.5	222.9

Figure 10. $^{31}P\{^1H\}$ NMR data for mono- and dinuclear Rh complexes with SPANphos and pySPAN ligands.

Although the different electronic character of the bispyrrolylphosphine ligand results in downfield-shifted signals and larger coupling constants, according to the spectroscopic pattern, the reactivity of SPANphos and pySPAN with $[Rh(CO)_2Cl]_2$ is essentially the same. The mononuclear complexes show the typical ABX spectrum due to the diastereotopic phosphorus nuclei, but in dinuclear compounds, the two phosphorus nuclei are equivalent due to the C_2 symmetry of the molecule.

It is well-known that the coordination mode of the phosphines (either ee or ea, bisequatorial or equatorial-apical) in the active hydroformylation catalyst $[RhH(CO)_2(L)]$ (L = chelating diphosphine) is crucial in determining the selectivity of this reaction.[54] To analyze the preferred coordination mode of SPANphos on a related five-coordinated rhodium center,[55] the ligand was reacted with 1 equiv of $[RhH(CO)(PPh_3)_3]$ in CD_2Cl_2. As shown in Figure 11, the reaction is shifted toward the right-hand side of the equation, although some starting complex and free ligand remained unreacted. The spectrum could be simulated using an ABCX (P,P,P,Rh) spin system with the data shown in Figure 11. Both the spin system and the coupling constants observed are in agreement with the species $[RhH(CO)(PPh_3)(SPANphos)]$, with all three phosphoruses occupying equatorial positions in the trigonal bipyramidal complex. Nevertheless, it is not possible to confirm wether it is the expected monometallic chelate, a bimetallic structure with the SPANphos ligand acting as a double bridge or a species with two SPANphos ligands coordinated in monodentate manner because all three species could show identical NMR spectroscopic patterns.

To study the coordination properties of SPAN-based ligands in the real complexes used in the hydroformylation experiments, solutions of SPANphos and pySPAN and $[Rh(CO)_2(acac)]$ in toluene-d_8 were poured in a high pressure NMR sapphire tube and analyzed under argon and under 20 bar of syngas pressure (Figure 12).

Under an argon atmosphere, the $^{31}P\{^1H\}$ NMR spectra showed in both cases a phosphorus signal at low field as a doublet (δ = 42.2 ppm for SPANphos, δ = 100.3 ppm for pySPAN). Notably, the coupling constant $^1J_{P-Rh}$ was significantly higher for the more π-accepting pySPAN (175 vs 222 Hz). A second rather broad signal appeared at chemical shifts close to those of free ligands, suggesting the presence of noncoordinated phosphorus. It is not clear in which exchange process this phosphorus atom may be involved, but these features suggest that in both cases, a complex of the type $[Rh(acac)(CO)_2(P-P)]$ **A** is formed, in which the ligand is acting in a monodentate manner.

When a pressure of 20 bar syngas was applied to these solutions and they were kept at 80 °C for 2 h (simulating incubation conditions employed in hydroformylation experiments) the $^{31}P\{^1H\}$ NMR spectra changed significantly. In both cases, the signal due to species **A** completely disappeared, and a new doublet was observed (δ = 33.3 ppm for SPANphos, δ = 98.7 ppm for pySPAN). Here again, the coupling constant was larger for the more π-accepting pySPAN (144 vs 198 Hz). This observation suggests that both phosphorus nuclei of the SPAN ligand became equivalent on the NMR time scale.

In the case of SPANphos, a second signal was detected at +21.0 ppm (second-order signal, $^1J_{P-Rh}$ = 121 and $^2J_{P-Rh}$ = −5 Hz, approximate values) along with a broad peak at chemical shift close to the one of the free ligand (−14.8 ppm). The small signal at +21 ppm is typical of dimeric species, suggesting the presence of a side product that has a bimetallic bridged structure.[56−61] Importantly, this species (denoted as **C**) was obtained as the major product when a pressure of 20 bar of only CO was applied. gNMR simmulation of this signal is in concordance with an A_2X (P_2Rh) spin system, suggesting that the species could be a dimer bearing two monocoordinated ligands (see the Suporting Information). These types of CO-bridged dimeric species are often observed in HP-NMR experiments[40,56] because of the relatively high concetrations required, but their presence at catalytic (mM) concentrations is often negligible.

^1H NMR spectra display a hydride signal around −9.5 ppm, being a triplet of doublets in each case (Table 2). These signals are typical of an equatorial−equatorial (e,e) ligand coordination mode, in the active hydroformylation species $[RhH(CO)_2(P)_2]$. To gain more information about species B-SPANphos, ^{13}C NMR spectra were recorded using a ^{13}C-enriched syngas mixture. A pseudo-quadruplet of doublets was detected at 200.9 ppm, suggesting that both CO ligands are equivalent on the NMR time scale. The set of coupling constants $^1J_{C-Rh}$, $^2J_{C-P}$, $^2J_{C-H}$ is formally a doublet of triplets of doublets ($^1J_{C-Rh}$ = 62.1 Hz;

dx.doi.org/10.1021/cs300470u | ACS Catal. 2013, 3, 128−137

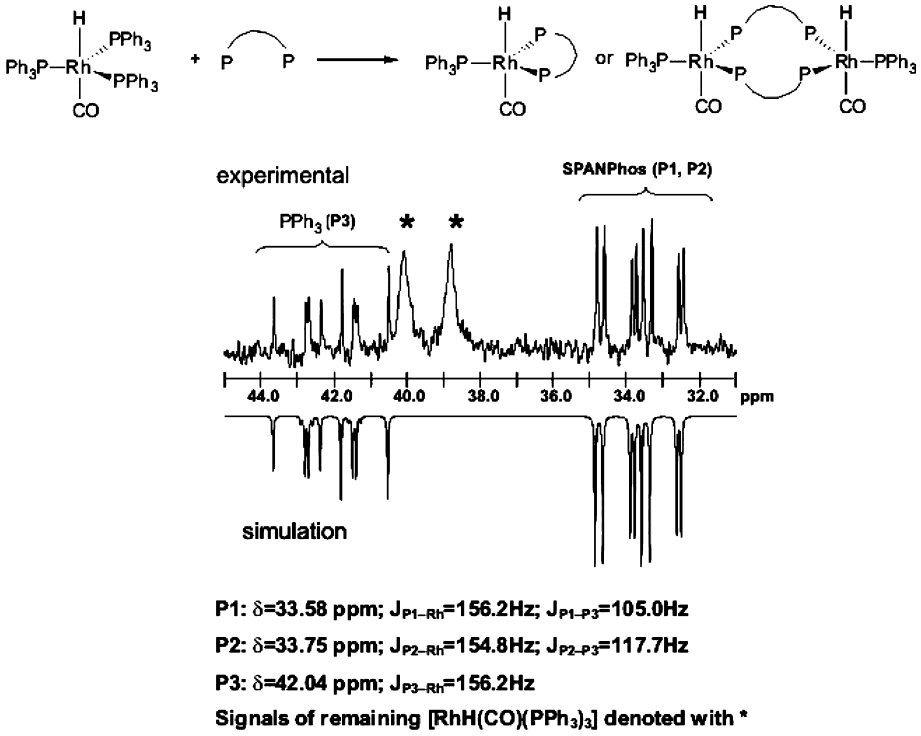

Figure 11. $^{31}P\{^1H\}$ spectrum of the reaction between $RhH(CO)(PPh_3)_3$ and SPANphos in CD_2Cl_2.

Ligand	A	B	C
pySPAN	**100.3** (d, $^1J_{P\text{-}Rh}$ = 222), **71.6** (s)	**98.7** (d, $^1J_{P\text{-}Rh}$ = 198)	not formed
SPANphos	**42.2** (d, $^1J_{P\text{-}Rh}$ = 175) **-14.8** (s)	**33.3** (d, $^1J_{P\text{-}Rh}$ = 144)	**21.0** (d, $^1J_{P\text{-}Rh}$ = 115, $J_{P\text{-}P}$ = 11) **-14.8** (bs)

Figure 12. $^{31}P\{^1H\}$ HPNMR (ppm). Chemical shifts in parts per million, coupling constants in hertz.

Table 2. ^1H and $^{13}C\{^1H\}$ HPNMR of Compounds B (ppm)[a]

complex	^1H	$^{13}C\{^1H\}$[b]
B-SPANphos	−9.5 (td, $^2J_{P-H}$ = 6.2, $^1J_{Rh-H}$ = 3.7)	200.9 (pseudo qd, $^1J_{C-Rh}$ = 62.1, ^2J = 12.6).
B-pySPAN	−9.5 (td, $^2J_{P-H}$ = 2.0, $^1J_{Rh-H}$ = 0.7)	not determined

[a]Chemical shifts in parts per million, coupling constants in hertz. [b]$^{13}C\{^1H\}$ HPNMR was obtained using an enriched $^{13}CO/H_2$ mixture.

$^2J_{C-P}$ and $^2J_{C-H}$ have similar values of ∼12.6 Hz). It is well documented that the exchange of an equatorial and an apical CO molecule in such a complex is very fast;[62,63] thus, the observed coupling constant $^1J_{C-Rh}$ is actually an average value between $^1J_{Cax-Rh}$ and $^1J_{Ceq-Rh}$.

The NMR data, especially the values of the observed coupling constants, are in agreement with a predominant formation of an equatorial-equatorial coordinated species **B**, but often ee and ea isomers are in equilibria on the NMR-time scale. To quantify the presence of bis-equatorial species under catalytic conditions (mM concentrations), HP-FTIR experiments were performed under 20 bar of syngas at 80 °C. In the case of SPANphos (Figure 13), the precursor $[Rh(CO)_2(acac)]$ rapidly disappears (ν_{CO} = 2082 and 2013 cm−1), and five new bands were observed at 2039, 2027, 2005, 1978, and 1949 cm^{-1}. The bands at 2027 and 1978 account for complex ee-$[RhH(CO)_2(P)_2]$, whereas the three other bands cannot be assigned with certainty. At this high dilution, CO-bridged dimers are not expected in high concentration (no signal accounting for bridging CO was detected around 1800 cm^{-1}), but no signals of an ea-isomer are observed.

HPIR experiments were also performed using pySPAN as a ligand (Figure 14). In this case, the bands of the Rh precursor (2082, 2013 cm^{-1}) are smoothly shifted over 90 min to reveal two unique carbonyl absorption bands (2063, 2009 cm^{-1}) under hydroformylation conditions. According to computational and experimental work on diphosphites,[64] the bands observed for Rh/pySPAN correspond to the bis-equatorial ee-$[RhH(CO)_2(P)_2]$ complex. This result, together with the NMR evidence, confirms that in the case of pySPAN, an ee-coordinated species of the type $[RhH(CO)(P)_2]$ is the only compound formed under catalytic conditions in the absence of substrate.

Thus, despite the similarity of the structure of the two ligands and their similar coordination chemistry to rhodium in square planar environments, the observed species under hydroformylation conditions are rather different: whereas SPANphos led to a mixture of rhodium−carbonyl complexes, the more π-accepting pySPAN favors the exclusive formation of one bis-equatorial complex. Nevertheless, in none of these experiments is it possible to distinguish if it is a chelating mononuclear or a dimeric structure with a double-bridging ligand, both with ee coordinated phosphor atoms (as expected for such bulky ligands).

HPIR experiments confirm in both cases that the ea isomer is not present under these conditions. Therefore, the surprising low regioselectivies obtained with these derivatives could be attributed to a dimeric nature of the active species **B**. It is also

dx.doi.org/10.1021/cs300470u | ACS Catal. 2013, 3, 128−137

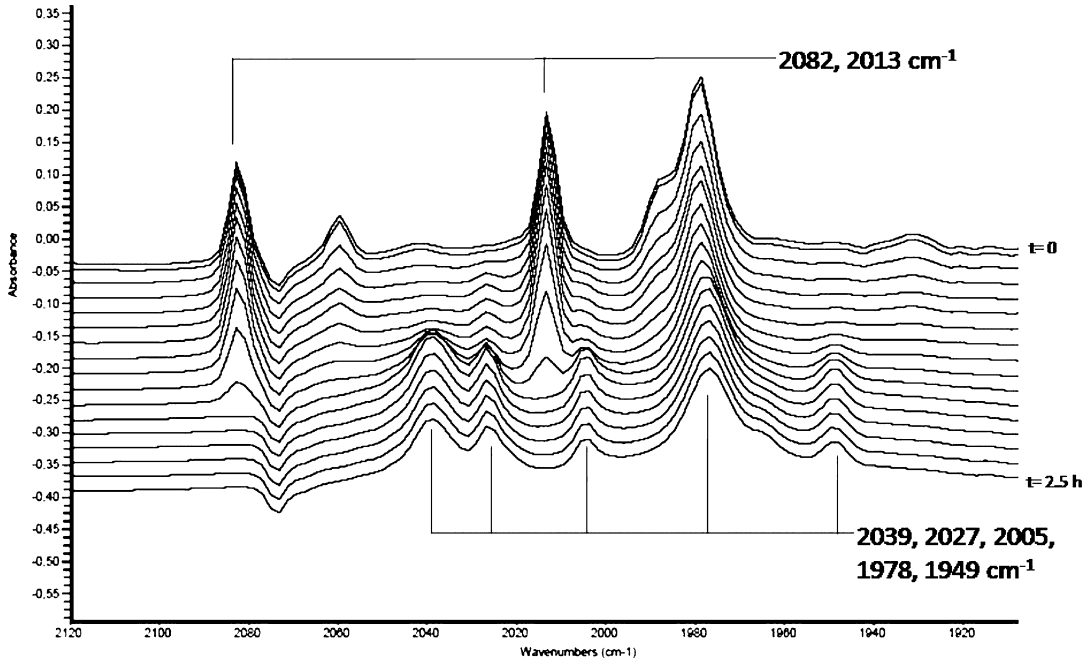

Figure 13. HP-FTIR experiment conditions using SPANphos. [Rh] = 2.6 mM, SPANphos/Rh = 2 in cyclohexane. Mixture pressurized at 20 bar of syngas and heated to 80 °C.

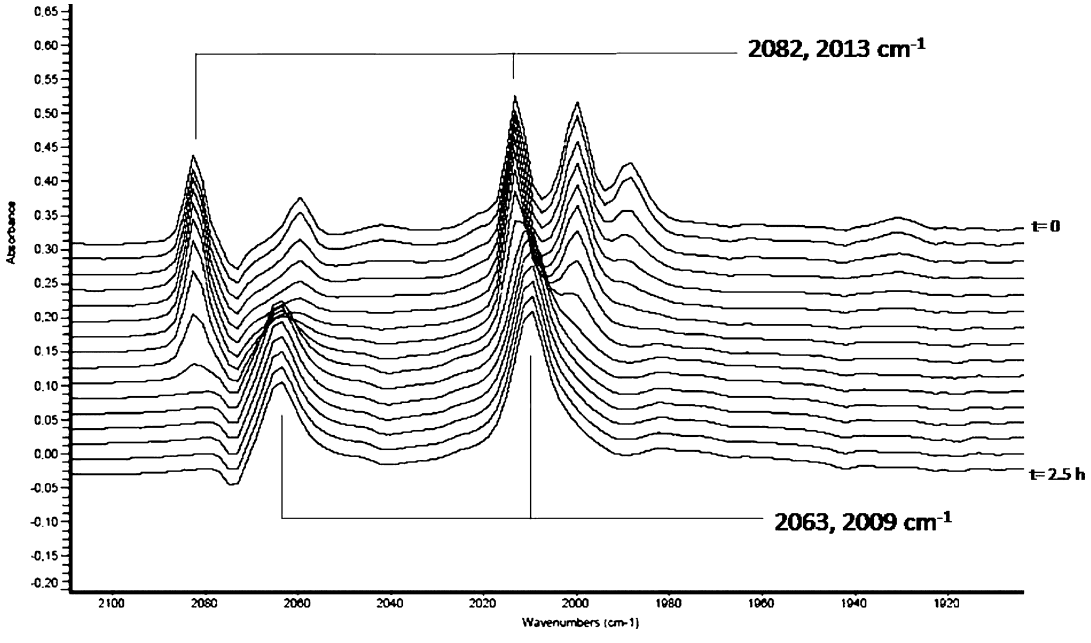

Figure 14. HP-FTIR experiment conditions using PySPAN: [Rh] = 2.6 mM, PySPAN/Rh = 2 in cyclohexane. Mixture pressurized at 20 bar of syngas and heated to 80 °C.

possible that in the case of SPANphos, an equilibrium between monodentate and bridging bimetallic species occurs. The electronic difference between the two ligands is held responsible for this important difference in coordination mode.

Ligands Having Xanthene Backbones. The phenyl analogue of pyXANT, Xantphos, has been reported to form a mixture of bis-equatorial ee and equatorial-apical ea rhodium complexes under hydroformylation conditions. As mentioned before, $^{31}P\{^{1}H\}$ HPNMR gave just one set of signals as a result of a fast exchange on the NMR time scale. This equilibrium can be quantified by HPIR spectroscopy by the intensities of the carbonyl stretching bands at 2039, 1996, 1974, and 1949 cm^{-1}.[65] Since previous studies on Rh/pySPAN catalyst revealed the existence of bis-equatorial Rh complexes as the unique species, the same analysis was performed with the Rh/pyXANT system (Figure 15).

The spectra reveal a rapid transition of the Rh precursor to the active species, characterized by four bands at 2063, 2005, 1980, 1974 cm^{-1}. The number of bands suggests the presence of a mixture of ee and ea complexes. Interestingly, the two bands at higher frequency appear at approximately the same wave numbers as those of Rh/pySPAN (Figure 14). To assign the four different bands observed for Rh/pyXANT to ee and ea isomers, another experiment involving deuterated syngas

dx.doi.org/10.1021/cs300470u | ACS Catal. 2013, 3, 128−137

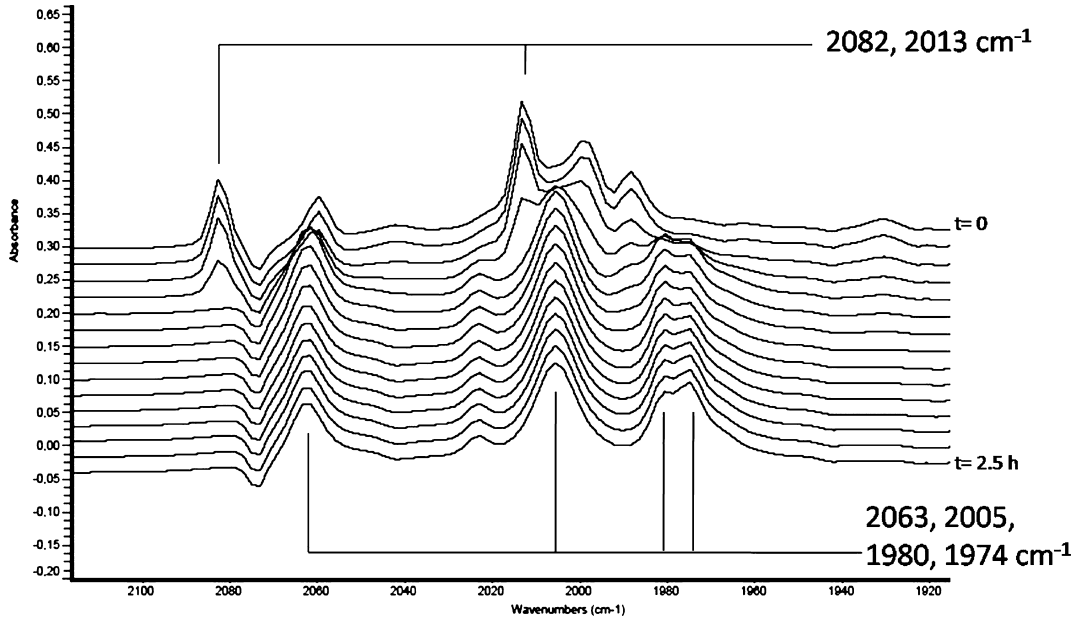

Figure 15. HP-FTIR experimental conditions using PyXANT. [Rh] = 2.6 mM, PyXANT/Rh = 2 in cyclohexane. Mixture pressurized at 20 bar of syngas and heated to 80 °C.

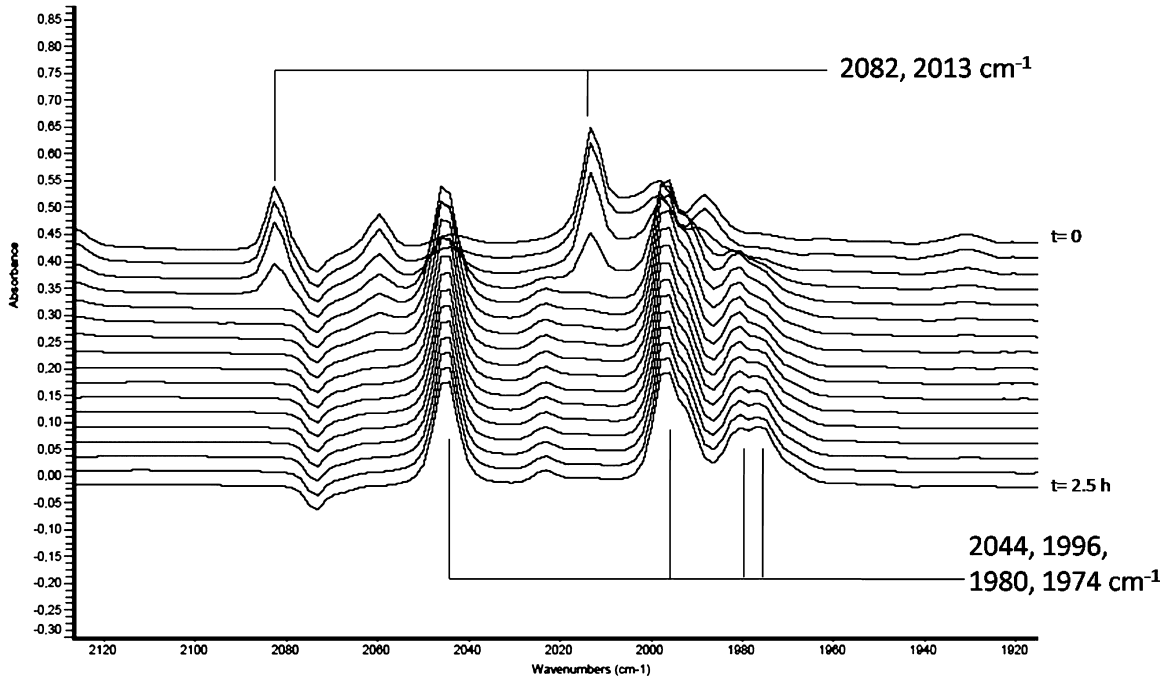

Figure 16. HP-FTIR experimental conditions using pyXANT. [Rh] = 2.6 mM, PyXANT/Rh = 2 in cyclohexane. Mixture pressurized at 20 bar of CO/D_2 and heated to 80 °C.

(CO/D_2) was performed to reveal the spectra shown in Figure 16.

As expected, only two of the CO absorptions were shifted to lower wave numbers when D_2 was used. Since the bands corresponding to ea species are not expected to change,[40] the signals at 1980 and 1974 cm^{-1} observed in Figures 13 and 14 correspond to the ea isomer, whereas the other bands at high wave numbers correspond to the predominant ee species. In this case, both isomers are attributed to chelate compounds of the type $[RhH(CO)_2(P{-}P)]$, as is well established for xanthene-based ligands. The preferential formation of the ee isomer is responsible in this case for the high regioselectivities observed in 1-octene hydroformylation.

CONCLUSION

We described here the synthesis of pyrrolyl-based monodentate and bidentate ligands. These strong π-acceptor ligands were investigated in the rhodium-catalyzed hydroformylation of ethene. Most of the ligands display activity exceeding for many of them the activity displayed by triphenylphosphine. This proves the better suitability of π-accepting ligands for this transformation. Phosphines substituted by pyrrole groups were more active than

dx.doi.org/10.1021/cs300470u | ACS Catal. 2013, 3, 128−137

those substituted with carbazole moieties. In particular, tri(pyrrolyl)phosphine, **L9**, showed unprecedented activity, reaching turnover frequencies up to 29.6×10^3 h^{-1}.

The influence of pyrrolyl-substituted bidentate ligands was also investigated. Again, in this case, they showed enhanced activity compared with their parent phenyl-substituted one. Both pyXANT and pySPAN displayed very high activity. It is noteworthy that all these catalytic systems proved to be very selective, propanal being the only hydroformylation product formed. pySPAN and pyXANT were also tested in 1-octene hydroformylation and proved to outperform SPANphos and Xantphos in terms of activity and regioselectivity

HPIR and HPNMR experiments allowed detection and characterization of ee isomers of the active species [HRh(CO)$_2$(**L**)]. In particular, the ligand pySPAN forms exclusively the ee isomer under hydroformylation conditions, whereas pyXANT forms a mixture of isomers. Under hydroformylation conditions, unidentified Rh complexes were detected as side-products in addition to the expected HRh(diphosphine)(CO)$_2$ that was detected when SPANphos was used as the ligand.

Hydrolysis tests performed on a model ligand showed the relative stability of these ligands toward water. Under acidic conditions, however, the decomposition is fast.

EXPERIMENTAL SECTION

Commercially available reactants were purchased from Aldrich, Acros, or Strem and were used as received. All reactions were carried out under an argon atmosphere using Schlenk techniques and SPS dried solvents. Deuterated chloroform was distilled over phosphorus pentoxide under argon prior to use. NMR spectra were recorded on a Bruker 400 MHz spectrometer. Chemical shifts are reported in parts per million and were calibrated using residual ^{1}H and ^{13}C resonances of deuterated solvents. Coupling constants (J) are expressed in hertz. Hydroformylation experiments were performed in a semiautomatic autoclave (AMTEC, Slurry phase reactor, SPR16) equipped with 16 stainless steel 15 mL reactors. All reactors were connected via a valve system with the gas supply and were equipped with individually adjustable stirring and heating. Rate data are reproducible within 5%. High-pressure IR experiments were performed in a 50 mL autoclave (SS 316) equipped with IRTRAN windows (ZnS), a mechanical stirrer, a temperature controller, and a pressure transducer.[14] IR spectra were recorded on a FTIR Nicolet 5700 Thermo spectrometer.

L5,[66] **L7**,[17] **L8**,[67] **L9**,[24] **L10**[67] and pyXANT[37] were synthesized according to literature procedures. Synthesis of ligands **L1**−**4**, **L6**, and pySPAN are described in the Supporting Information.

General Procedure for Ethene Hydroformylation Experiment. In a glovebox, in a test tube fitted with a septum were added [Rh(CO)$_2$(acac)], the ligand, toluene, and decane (internal standard with GC). The solution (5 mL) was then injected in the high pressure reactor under a nitrogen stream. The catalyst preformation was performed at 80 °C for 90 min under a pressure of 20 bar of syngas. After this time, the gases are vented and replaced with 20 bar of a ethene/CO/H$_2$ mixture at a ratio of 1:1:1. The turnover frequency is estimated by gas consumption. At the end of the reaction, the selectivity was measured by gas chromatography. Each reported value is the average of at least two experiments.

General Procedure for 1-Octene Hydroformylation Experiment. In a glovebox, a toluene solution of [Rh(CO)$_2$(acac)] and the ligand was prepared. The solution was then injected in the high pressure reactor under a nitrogen stream. The catalyst preformation was performed at 80 °C for 90 min under a pressure of 10 bar of syngas. After this time, a solution of 1-octene (5 mL) and decane (internal standard with GC) in toluene was injected into the reactor under preformation conditions, and the pressure of the syngas was increased to 20 bar. The mixture composition was determined by gas chromatography, and the initial turnover frequencies were estimated by gas consumption. Each reported value is the average of at least two experiments.

Procedure for HPNMR Experiment. In a glovebox, a high pressure NMR tube was filled with a solution of [Rh(CO)$_2$(acac)] (5 μmol in 0.1 mL toluene-d_8) and a solution of pySPAN (10 μmol in 0.1 mL toluene-d_8). ^{31}P{^{1}H} and ^{1}H NMR were measured first under an atmospheric pressure of argon on a Bruker 500 MHz spectrometer. The tube was then purged three times with cycles of 20−1 bar of syngas and shaken when the tube was at low pressure. Finally, the tube was charged with 20 bar of syngas and then heated to 80 °C for 2 h in the NMR probe to ensure complete formation of the complex. ^{31}P{^{1}H} and ^{1}H NMR were measured at variable temperatures.

ASSOCIATED CONTENT

Supporting Information

Synthetic procedures, NMR spectra, NMR simulation data. This material is available free of charge via the Internet at http://pubs.acs.org. CCDC 891787 contains the supplementary crystallographic data for this paper. These data can be obtained free of charge from the Cambridge Crystallographic Data Centre via www.ccdc.cam.ac.uk/data_request/cif.

AUTHOR INFORMATION

Corresponding Author

*E-mail: pvanleeuwen@iciq.es.

Present Addresses

‡BASF Española S. L. Catalysis Plant, 43006 Tarragona, Spain.

§Ikerbasque Research Professor, Departamento de Química Aplicada, Facultad de Ciencias Químicas, Universidad del País Vasco UPV-EHU, Apdo. 1072, 20080 San Sebastián, Spain.

Notes

The authors declare no competing financial interest.

ACKNOWLEDGMENTS

Dow Chemical Company is acknowledged for financial support. We thank Dr. Marta Martínez-Belmonte and Dr. Eduardo C. Escudero-Adán for solving the crystal structure and the ICIQ Research Support Units for their help and advice.

REFERENCES

(1) Evans, D.; Yagupsky, G.; Wilkinson, G. *J. Chem. Soc.* **1968**, 2660−2665.

(2) Brown, C. K.; Wilkinson, G. *J. Chem. Soc. A* **1970**, 2753−5764.

(3) Heck, R. F.; Breslow, D. S. *J. Am. Chem. Soc.* **1961**, *83*, 4023−4027.

(4) van der Veen, L. A.; Kamer, P. C. J.; van Leeuwen, P. W. N. M. *Organometallics* **1999**, *18*, 4765−4777.

(5) Gillespie, J.; Doods, D.; Kamer, P. C. J. *Dalton Trans.* **2010**, *39*, 2751−2764.

(6) van der Veen, L.; Keeven, P. H.; Schoemaker, G. C.; Reek, J. N. H.; Kamer, P. C. J.; van Leeuwen, P. W. N. M.; Lutz, M.; Spek, A. L. *Organometallics* **2000**, *19*, 872−883.

(7) Slagt, V. F.; Reek, J. N. H.; Kamer, P. C. J.; van Leeuwen, P. W. N. M. *Angew. Chem., Int. Ed.* **2001**, *40*, 4271−4274.

(8) Bellini, R.; Chikkali, S. H.; Bethon−Gelloz, G.; Reek, J. N. H. *Angew. Chem., Int. Ed.* **2011**, *50*, 7342−7345.
(9) Kamer, P. C. J.; Reek, J. N. H.; van Leeuwen, P. W. N. M. Rhodium Catalyzed Hydroformylation. In *Catalysis by Metal Complexes*; van Leeuwen, P. W. N. M.; Claver, C., Eds.; Kluwer, Dordrecht, 2000, Vol. *22*, pp 35−62 and references therein.
(10) Pruett, R. L.; Smith, J. A. *J. Org. Chem.* **1969**, *34*, 327−330.
(11) van Leeuwen, P. W. N. M.; Roobeek, C. F. *J. Organomet. Chem.* **1983**, *258*, 343−350.
(12) Billig, E.; Abatjoglou, A. G.; Bryant, D. R. U.S. Patents 4,769,498, 4,668,651, 4748261, 1987, to Union Carbide Corp.
(13) van Rooy, A.; Orij, E. N.; Kamer, P. C. J.; van Aardweg, F.; van Leeuwen, P. W. N. M. *Chem. Commun.* **1991**, 1096−1097.
(14) van Rooy, A.; Orij, E. N.; Kamer, P. C. J.; van Leeuwen, P. W. N. M. *Organometallics* **1995**, *14*, 34−43.
(15) Tricas, H.; Diebolt, O.; van Leeuwen, P. W. N. M. *J. Catal.* **2013**, accepted.
(16) Märkl, G. *Angew. Chem., Int. Ed.* **1966**, *78*, 907−908.
(17) Vogt, D.; Müller, C. *Dalton Trans.* **2007**, 5505−5523.
(18) Mézailles, N.; Le Floch, P. *Curr. Org. Chem.* **2006**, *10*, 3−25.
(19) Moloy, K. G.; Petersen, J. L. *J. Am. Chem. Soc.* **1995**, *117*, 7696−7710.
(20) Burrows, A. D.; Kociok-Köhn, G.; Mahon, M. F.; Varrone, M. *C. R. Chim.* **2006**, *9*, 111−119.
(21) Breit, B.; Winde, R.; Mackewitz, T.; Paciello, R.; Harms, K. *Chem.—Eur. J.* **2001**, *7*, 3106−3121.
(22) Breit, B. *Chem. Commun.* **1996**, 2071−2072.
(23) van der Slot, S. C.; Duran, J.; Luten, J.; Kamer, P. C. J.; van Leeuwen, P. W. N. M. *Organometallics* **2002**, *21*, 3873−3883.
(24) Jackstell, R.; Klein, H.; Beller, M.; Wiese, K.-D.; Röttger, D. *Eur. J. Org. Chem.* **2001**, 3871−3877.
(25) Yu, S.; Chie, Y.-m.; Guan, Z.-h.; Zou, Y.; Li, W.; Zhang, X. *Org. Lett.* **2009**, *11*, 241−244.
(26) Trzeciak, A. M.; Glowiak, T.; Grybek, R.; Ziólkowski, J. *J. Chem. Soc., Dalton Trans.* **1997**, 1831−1837.
(27) Naili, S.; Mortreux, A.; Agbossou, F. *Tetrahedron Asymmetry* **1998**, 3421−3430.
(28) Yan, Y.; Zhang, X.; Zhang, X. *J. Am. Chem. Soc.* **2006**, *128*, 16058−16062.
(29) Cai, C.; Yu, S.; Cao, B.; Zhang, X. *Chem.—Eur. J.* **2012**, *18*, 9992−9998.
(30) Mo, M.; Yi, T.; Zheng, C.-Y.; Yuan, M.-L.; Fu, H.-Y.; Li, R.-X.; Chen, H. *Catal. Lett.* **2012**, *142*, 238−242.
(31) Hamers, B.; Kosciusko-Morizet, E.; Müller, C.; Vogt, D. *ChemCatChem* **2009**, *1*, 103−106.
(32) MacDougall, J. K.; Simpson, M. C.; Green, M. J.; Cole-Hamilton, D. J. *Dalton Trans.* **1996**, 1161−1172.
(33) Deshpande, R. M.; Bhanage, B., M.; Divekar, S. S.; Kanagasabapathy, S.; Chaudhari, R. V. *Ing. Eng. Chem. Res.* **1998**, *37*, 2391−2396.
(34) Zhang, J.; Poliakoff, M.; George, M. W. *Organometallics* **2003**, *22*, 1612−1618.
(35) Li, C.; Gui, L.; Garland, M. *Organometallics* **2004**, *23*, 2201−2204.
(36) Note that **L1**−**L6** bear bisphenol substituents similar to the successful Union Carbide phosphite ligands: Billig, E.; Abatjoglou, A. G.; Bryant, D. R.; Murray, R. E.; Maher, J. M. U.S. Patent 4,599,206, 1986, to Union Carbide Corp.
(37) Kranenburg, M.; van der Burgt, Y. E. M.; Kamer, P. C. J.; van Leeuwen, P. W. N. M. *Organometallics* **1995**, *14*, 3081−3089.
(38) Freixa, Z.; Beentjes, M. S.; Batema, G. D.; Dieleman, C. B.; van Strijdonk, G. P. F.; Reek, J. N. H.; Kamer, P. C. J.; Fraanje, J.; Goubitz, K.; van Leeuwen, P. W. N. M. *Angew. Chem., Int. Ed.* **2003**, *42*, 1284−1287.
(39) Ahlers, W.; Paciello, R.; Vogt, D.; Hofmann, P. WO02083695, U.S. patent 2004110960, 2002, to BASF.
(40) Rafter, E.; Gilheany, D. G.; Reek, J. N. H.; van Leeuwen, P. W. N. M. *ChemCatChem* **2010**, *2*, 387−391.
(41) Casey, C. P.; Whiteker, G. T.; Melville, M. G.; Petrovich, L. M.; Gavney, J. A., Jr.; Powell, D. R. *J. Am. Chem. Soc.* **1992**, *114*, 5535−5543.
(42) Kranenburg, M.; van der Burgt, Y. E. M.; Kamer, P. C. J.; van Leeuwen, P. W. N. M.; Goubitz, K.; Fraanje, J. *Organometallics* **1995**, *14*, 3081−3089.
(43) Van der Veen, L. A.; Boele, M. D. K.; Bregman, F. R.; Kamer, P. C. J.; van Leeuwen, P. W. N. M.; Goubitz, K.; Fraanje, J.; Schenk, H.; Bo, C. *J. Am. Chem. Soc.* **1998**, *120*, 11616−11626.
(44) van der Veen, L. A.; Kamer, P. C. J.; van Leeuwen, P. W. N. M. *Angew. Chem., Int. Ed.* **1999**, *38*, 336−338.
(45) Paciello, R.; Siggel, L.; Röer, M. *Angew. Chem., Int. Ed.* **1999**, *38*, 1920−1923.
(46) Breit, B.; Seiche, W. *Angew. Chem., Int. Ed.* **2005**, *44*, 1640−1643.
(47) Slagt, V. F.; van Leeuwen, P. W. N. M.; Reek, J. N. H. *Angew. Chem., Int. Ed.* **2003**, *42*, 5619−5623.
(48) Kuil, M.; Soltner, T.; van Leeuwen, P. W. N. M.; Reek, J. N. H. *J. Am. Chem. Soc.* **2006**, *128*, 11344−11345.
(49) Bronger, R. P. J.; Silva, S. M.; Kamer, P. C. J.; van Leeuwen, P. W. N. M. *Dalton Trans.* **2004**, 1590−1596.
(50) Bronger, R. P. J.; Kamer, P. C. J.; Van Leeuwen, P. W. N. M. *Organometallics* **2003**, *22*, 5358−5369.
(51) Trzeciak, A. M.; Glowiak, T.; Grzybek, R.; Ziolkowski, J. J. *J. Chem. Soc., Dalton Trans.* **1997**, 1831−1838.
(52) van Leeuwen, P. W. N. M.; Chadwick, J. C. *Homogeneous Catalysts: Activity, Stability, Deactivation*; Wiley-VCH: Weinheim, Germany, 2011.
(53) Freixa, Z.; Kamer, P. C. J.; Spek, A. L.; van Leeuwen, P. W. N. M. *Angew. Chem., Int. Ed.* **2005**, *44*, 4385−4388.
(54) Freixa, Z.; van Leeuwen, P. W. N. M. *Dalton Trans.* **2003**, 1890−1901.
(55) It was shown earlier that the high flexibility range of SPANphos ligand can allow the formation of a 4-coordinated rhodium complex, SPANphos being coordinated in a cis fashion: Jiménez-Rodríguez, C.; Roca, F. X.; Bo, C.; Benet-Buchholz, J.; Escudero-Adán, E. C.; Freixa, Z.; van Leeuwen, P. W. N. M. *Dalton Trans.* **2006**, 268−278.
(56) Evans, D.; Yagupsky, G.; Wilkinson, G. *J. Chem. Soc. A* **1968**, 2660−2665.
(57) Chan, A. S. C.; Shieh, H. S.; Hill, J. R. *J. Chem. Soc., Chem. Commun.* **1983**, 688−689.
(58) James, B. R.; Mahajan, D.; Rettig, S.J .; Williams, G. M. *Organometallics* **1983**, *2*, 1452−1458.
(59) Moasser, B.; Gladfelter, W. L.; Roe, C. D. *Organometallics* **1995**, *14*, 3832−3838.
(60) Buisman, G. J. H.; van der Veen, L. A.; Kamer, P. C. J.; van Leeuwen, P. W. N. M. *Organometallics* **1997**, *16*, 5681−5687.
(61) Castellanos-Paez, A.; Castillon, S.; Claver, C.; van Leeuwen, P. W. N. M.; de Lange, W. G. J. *Organometallics* **1998**, *17*, 2543−2552.
(62) Kamer, P. C. J.; Reek, J. N. H.; van Leeuwen, P. W. N. M. in *Mechanisms in Homogeneous Catalysis; A Spectroscopic approach*; Heaton, B., Ed.; Wiley VCH: Weinheim, 2005, pp 231−270.
(63) van der Slot, S.; Kamer, P. C. J.; van Leeuwen, P. W. N. M.; Iggo, J. A.; Heaton, B. T. *Organometallics* **2001**, *20*, 430−441.
(64) Selent, C.; Franke, R.; Kubis, C.; Spannenberg, A.; Baumann, W.; Kreidler, B.; Börner, A. *Organometallics* **2011**, *30*, 4509−4514.
(65) Zuidema, E.; Goudriaan, P. E.; Swennenhuis, B. H. G.; Kamer, P. C. J.; van Leeuwen, P. W. N. M.; Lutz, M.; Spek, A. L. *Organometallics* **2010**, *29*, 1210−1221.
(66) Ljungdahl, N.; Pera, N. P.; Andersson, K. H. O.; Kann, N. *Synlett* **2008**, 394−398.
(67) Burrows, A. D.; Mahon, M. F.; Varrone, M. *Dalton Trans.* **2004**, 3321−3330.